JOURNAL OF MATERIALS SCIENCE **35** (2000) 4685–4693

Damage development under gradual loading of composites

F. KUN*
Institute for Computer Applications (ICA1), University of Stuttgart, Pfaffenwaldring 27, D-70569 Stuttgart, Germany; Department of Theoretical Physics, Kossuth Lajos University, P.O.Box: 5, H-4010 Debrecen, Hungary
E-mail: feri@ica1.uni-stuttgart.de

H. J. HERRMANN
Institute for Computer Applications (ICA1), University of Stuttgart, Pfaffenwaldring 27, D-70569 Stuttgart, Germany

We present a theoretical investigation of damage development in Ceramic Matrix Composites (CMC's) before catastrophic failure under gradual loading conditions. The aim of the work is to give a theoretical interpretation of the experimental results on the development of damage in the C/C-SiC composite obtained by cyclically loading, unloading, and reloading a planar specimen. Our approach is based on statistical, micromechanical models of the failure of CMC's in the framework of global load sharing, where the failure mechanism includes quasi-periodic matrix cracking, gradual breaking of fibers, and sliding of broken fibers with respect to the matrix. It is demonstrated that the non-linear characteristics of the constitutive behavior and the potential drop measured under uniaxial loading of a planar C/C-SiC specimen can be described with reasonable accuracy in the framework of statistical, micromechanical models.

1. Introduction

Ceramic Matrix Composites (CMC's) have a great technological importance due to their good mass specific properties, good performance at high temperature and relatively low production costs. In the study of the failure of CMC's the main interest is in the strength distribution of the material and in the dependence of strength on the sample size [1–18]. The characterization of the damage state and damage development in CMC's before catastrophic failure under gradual loading conditions has also received much attention especially by the experimental community [18–29]. In the past decade a large amount of theoretical efforts have been devoted to the study of reliability and size scaling of composite's strength, and to clarify how the ultimate tensile strength depends on the underlying constituent properties of fibers, matrix and fiber-matrix interface [7–18]. Sophisticated numerical techniques have been developed which enable also large scale calculations of the strength of composites, and by now this problem is well understood [11–17]. However, much less is known about the behavior of CMS's before catastrophic failure occurs, under gradual (cyclic) loading conditions. A large amount of experimental results [18–29] have been accumulated over the past years but a comprehensive theoretical understanding is still lacking.

Recently, a conductivity (DC potential drop) based non-destructive test-method was developed for the purpose of damage state evaluation for composites, and it was applied to the carbon fiber reinforced carbon-silicon-carbide C/C-SiC composite [19]. Since the C/C-SiC is a candidate material to be used in aerospace applications and also in power plants for ultra high temperature heat exchangers, the evaluation of its damaged state is of crucial interest. In the manufacturing process of C/C-SiC liquid silicon is poured into a two-dimensional woven C/C-preform to form a silicon-carbide matrix in order to prevent the C fibers from oxidation. For a detailed description of the manufacturing process and for the mechanical properties of C/C-SiC see Ref. [19]. The most important characteristic quantities of C fibers and that of the composite are summarized in Table I.

The experiments were performed under stress-controlled conditions such that a planar C/C-SiC specimen was cyclically loaded, unloaded, and reloaded while a fixed electric current I_o was maintained between two cross sections of the specimen. To obtain information about the damage development under gradual loading, the macroscopic constitutive behavior $\sigma(\epsilon)$ and the potential drop U between the two sections of the specimen were monitored. Since the matrix material SiC practically does not contribute to the electric conductivity of the composite, the potential drop measurement provides direct information about the damage occurring in fibers and fiber bundles, while the

* Author to whom all correspondence should be addressed.

constitutive behavior contains also the complicated effect of the matrix and fiber-matrix interface. The most important experimental findings can be summarized as follows [19–24]: (a) The macroscopic constitutive behavior $\sigma(\epsilon)$ is non-linear with a decreasing unloading modulus. During the unloading-reloading sequences $\sigma(\epsilon)$ exhibits hysteresis with increasing opening. At complete unloading $\sigma = 0$ remaining anelastic strain ϵ_{an} occurs. (b) The difference ΔU of the potential drops $U(\epsilon)$ and U_o measured at a strain ϵ and at the initial state between two sections of the specimen, is a non-linearly increasing function of ϵ. It was found that $\Delta U(\epsilon)$ can be well fitted with a power law with an exponent between 1 and 2. During the unloading-reloading sequences hysteresis of ΔU with increasing opening occurs, and at complete unloading ΔU as a function of the anelastic strain ϵ_{an} can be well approximated by a straight line.

The aim of the present paper is to give a theoretical description of the experimental results on the damage development in C/C-SiC composite under uniaxial loading focusing on the constitutive behavior $\sigma(\epsilon)$ and on the potential drop $\Delta U(\epsilon)$ as a function of strain ϵ. Our approach is based on statistical, micromechanical models of composites's failure, which were recently studied in the context of size scaling of the global strength of composites [7–17]. In the formulation of the constitutive equations we build mainly upon the work of Phoenix and Raj [10], Curtin [15, 16], Hild *et al*. [25] and Weigel *et al*. [26]. The failure mechanism of our model captures quasi-periodic matrix cracking, gradual breaking of fibers and sliding of fibers relative to the matrix. We show that based on these simple assumptions in the framework of the global load sharing approach it is possible to explain the observed non-linear characteristics of the constitutive behavior and that of the potential drop. It has to be emphasized that our method of investigation is general, it can be applied to study damaging of other composites as well, and it can also serve as a basis for the formulation of material laws in the framework of continuum damage mechanics [25].

After giving a short summary of the main ideas of our modeling in Sec. 2, the constitutive equations of the material and the behavior of the potential drop will be derived in Secs. 3 and 4, respectively. In Sec. 5 we compare the results of the model calculations to the experimental ones. In Sec. 6 the limitations of our approach and possible future improvements will be discussed.

2. Modeling damage development

The evolution of damage and the tensile failure of fiber reinforced composites depends primarily on two factors, i.e. on the strength distribution of the individual fibers and on the mechanics of load transfer from broken fibers to the unbroken ones. The strength distribution of fibers can be well established a priori, but the details of the load transfer mechanism depend on many constituent properties and, in particular, on the detailed mechanics of the fiber-matrix interface. Hence, it is very difficult to obtain it correctly if more than one fiber is broken. Among the several theoretical approaches, one simplification that makes the problem analytically tractable is the assumption of Global Load Sharing (GLS), which means that after each fiber breaking the stress is equally distributed on the intact fibers neglecting stress enhancement in the vicinity of failed regions [1–10, 15–18]. This approach implies 'infinite' range interaction between fibers so it corresponds to a mean field approach. The other limiting case is applying Local Load Sharing (LLS), where the stress is redistributed in the vicinity of a failed fiber giving rise to high stress concentration around failed regions [6–8, 11–14].

It is reasonable to assume that when the C/C-SiC composite with woven structure is loaded parallel to one of the main fiber directions, the perpendicular fibers carry practically no load. That is why, as a first step of the model construction we neglect the woven structure and consider only an unidirectional ensemble of fibers. In the case of the C/C-SiC composite, due to the high residual stresses generated by thermal expansion mismatch and matrix porosity, the silicon carbide matrix is multiply cracked even during the manufacturing process [19]. Under elongation further cracks appear in the matrix perpendicular to the loading direction. It is verified experimentally that rather than propagating through the fibers, the fiber-matrix interface debonds and the fibers slide relative to the matrix with sliding resistance τ. This implies that over a length l_{m} the stress in the matrix builds up linearly to the original level giving rise to new cracking. Thus, it can be considered that after reaching a certain stress value σ_{mc} the matrix is quasi-periodically cracked and cannot support further load, therefore, all the additional load is carried by the fibers. In the experiments the Young-modulus of the woven carbon fiber network without the matrix material was found to be equal to the Young-modulus of the complete C/C-SiC composite [22, 23], which also supports the above argument.

In the following we show that based on these simple model assumptions in the framework of global load sharing it is possible to reproduce the qualitative behavior of the potential drop as a function of the load, and the macroscopic constitutive behavior of the C/C-SiC composite.

3. Loading-unloading-reloading sequences in the framework of GLS

In the derivation of the constitutive equations we follow the ideas presented in Refs. [10, 16, 25]. After the above simplifying assumptions, the system under consideration is composed of N parallel, cylindrical fibers with length L_{o}, radius r and cross section A_{fo}. Let us denote f the ratio of the total cross sectional area of the fibers and the total cross section of the specimen A_{o}, i.e. $f = NA_{fo}/A_{\text{o}}$ the volume fraction of fibers. The fibers are considered to be linearly elastic until breaking (brittle rupture) with identical Young-modulus E_f.

When a fiber breaks the load carried by the fiber drops down to zero at the position of the break. Similar to the case of matrix cracking, the fiber-matrix interface debonds and the stress builds up in the fiber through the stress transfer across the sliding fiber-matrix interface. During the loading process, the stress in a broken fiber

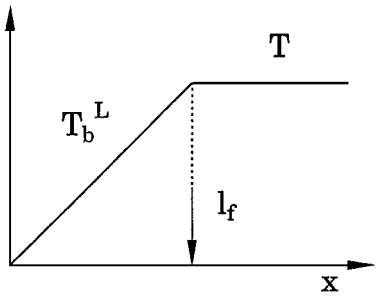

Figure 1 The stress T_b^L along a broken fiber under loading. The sliding length l_f is also indicated. The slope of T_b^L is $2\tau/r$.

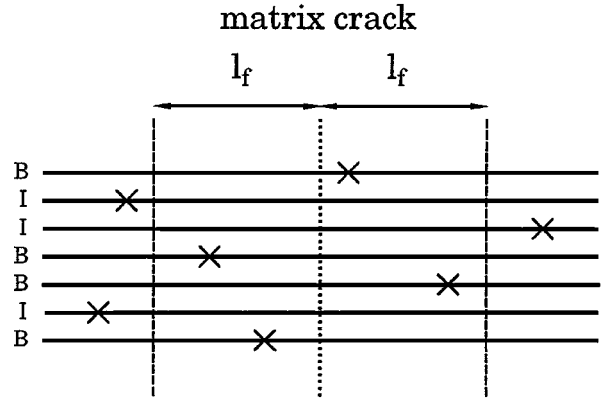

Figure 2 Illustration of the distribution of fiber breaks (crosses) in the vicinity of the reference matrix crack plane. Fibers which do not have a break within a distance l_f are considered to be intact (I), otherwise they are considered to be broken (B).

T_b^L as a function of the distance x from the break can be written as

$$T_b^L(x) = \frac{2\tau}{r}x, \tag{1}$$

where τ denotes the sliding resistance at the fiber matrix interface [16, 28, 30, 31]. The upper script L corresponds to the loading of the specimen. Equation 1 also implies that T_b^L reaches the stress value T of intact fibers at a sliding length $l_f = rT/2\tau$, as illustrated in Fig. 1.

For the statistical variation of fiber strength a Weibull distribution is assumed

$$P(T) = 1 - \exp\left[-\left(\frac{T}{\sigma_c}\right)^{m+1}\right], \tag{2}$$

where m denotes the Weibull modulus determining the variability of strength, and σ_c is the characteristic strength of fibers embedded in a matrix. The characteristic length scale δ_c associated to σ_c plays also a crucial role

$$\sigma_c = \left(\frac{l_o\sigma_o^m\tau}{r}\right)^{1/m+1}, \quad \delta_c = \left(\frac{\sigma_o r l_o^{1/m}}{\tau}\right)^{m/m+1}, \tag{3}$$

where l_o is the reference length, and σ_o is the characteristic strength of a single fiber of length l_o. Physically, δ_c is twice the sliding length around a fiber break that is required to attain the characteristic stress σ_c, and hence they satisfy the relation $\delta_c = r\sigma_c/\tau$ [16, 28]. This also implies that fiber breaks spaced by more than δ_c along the fiber direction do not influence each other directly, and consequently, regions of the composite separated longitudinally by more than δ_c are essentially independent of each other [12–16]. In Equation 2 $P(T)$ gives the cumulative probability that a fiber of characteristic length δ_c breaks for a load less than or equal to T.

For the formulation of the constitutive equations let us consider a matrix crack plane as reference. Here all the applied load is carried by fibers, hence, the average load per fiber is σ/f. Some of the fibers might be broken in the vicinity of the reference plane, that is why they can carry less stress than the average, which implies that the intact fibers have to pick up this excess load. *Global Load Sharing* means the assumption that the excess load due to fiber breaking is equally redistributed on all the intact fibers, and stress concentration around failed fibers is neglected. According to the above explanation, those fibers are considered to be intact which do not have a break within the distance $\pm l_f$ from the reference plane, however, the broken fibers carry also some load at the reference crack plane due to Equation 1, see also Fig. 2. When T denotes the average load on intact fibers, the general form of the constitutive equation reads as

$$\frac{\sigma}{f} = T(1 - P(T)) + \langle T_b\rangle P(T), \tag{4}$$

where $\langle T_b\rangle$ denotes the average stress carrying capacity of broken fibers within a distance l_f from the reference plane, $P(T)$ and $1 - P(T)$ are the fraction of broken and intact fibers, respectively [10, 15, 16]. Specific forms of the constitutive behavior for the case of loading, unloading and reloading can be obtained from Equation 4 by plugging in the proper form of $\langle T_b\rangle$.

In order to calculate the average stress carried by broken fibers $\langle T_b\rangle$, it is necessary to construct the probability distribution $f(x)$ of the distance x of a fiber break from the reference matrix crack plane, provided that a break occurs within a distance $\pm l_f$. For this conditional probability distribution Phoenix and Raj deduced the following form based on Weibull statistics [10]

$$f(x) = \frac{1}{P(T)l_f}\left(\frac{T}{\sigma_c}\right)^{m+1}\exp\left[-\left(\frac{x}{l_f}\right)\left(\frac{T}{\sigma_c}\right)^{m+1}\right], \tag{5}$$

where $x \in [0, l_f]$. Note that Phoenix and Raj [10] and Curtin [16] derived the constitutive behavior only for the case of loading. Hild *et al.* [25] used a unique distribution of x to obtain the constitutive equations for loading, unloading and reloading, furthermore, Weigel *et al.* applied also a different form of $f(x)$. In the following we derive constitutive equations based on the distribution given by Equation 5 for loading, unloading, and reloading of the specimen.

The averaging of T_b^L for the case of loading using Equation 5 leads to

$$\langle T_{\mathrm{b}}^{\mathrm{L}} \rangle = \int_0^{l_f} T_{\mathrm{b}}^{\mathrm{L}}(x) f(x)\,\mathrm{d}x = T\left[\left(\frac{\sigma_{\mathrm{c}}}{T}\right)^{m+1} - \frac{1-P(T)}{P(T)}\right], \quad (6)$$

and from Equation 4 the constitutive behavior for loading can be cast into the form

$$\frac{\sigma^{\mathrm{L}}}{f} = TP(T)\left(\frac{\sigma_{\mathrm{c}}}{T}\right)^{m+1} = E_f \epsilon^{\mathrm{L}} P(T)\left(\frac{\sigma_{\mathrm{c}}}{E_f \epsilon^{L}}\right)^{m+1}. \quad (7)$$

The upper script L corresponds to the loading of the specimen. To obtain the strain dependence of σ^{L} we applied that $T = E_f \epsilon^{\mathrm{L}}$, since the fibers are supposed to be linearly elastic, and due to the parallel coupling of fibers their average strain yields the strain of the composite. The Ultimate Tensile Strength σ_{UTS} is the value of σ^{L} at the maximum of $\sigma^{\mathrm{L}}(\epsilon^{\mathrm{L}})$ [10, 16, 25]. Here, the behavior of σ_{UTS} is not studied, we refer to the literature [10, 16].

When unloading the specimen, the stress distribution along broken fibers changes, since at the broken face of a fiber the sliding happens in the opposite direction giving rise to a stress distribution $T_{\mathrm{b}}^{\mathrm{U}}$ presented in Fig. 3 [25, 30]. We parameterize the unloading process with ΔT^{U} so that the actual stress level T^{U} in intact fibers is $T^{\mathrm{U}} = T_{\mathrm{M}} - \Delta T^{\mathrm{U}}$, where T_{M} denotes the maximal value of stress on intact fibers reached before the unloading sets in. ΔT^{U} varies between 0 and a maximal value T_{m}, discussed later. Averaging $T_{\mathrm{b}}^{\mathrm{U}}$ with Equation 5 yields

$$\langle T_{\mathrm{b}}^{\mathrm{U}} \rangle = \int_0^{l_f} T_{\mathrm{b}}^{\mathrm{U}}(x) f(x)\,\mathrm{d}x = \frac{2T_{\mathrm{M}}}{P(T_{\mathrm{M}})}\left(\frac{\sigma_{\mathrm{c}}}{T_{\mathrm{M}}}\right)^{m+1} \times \left\{ \exp\left[-\left(\frac{\Delta T^{\mathrm{U}}}{2T_{\mathrm{M}}}\right)\left(\frac{T_{\mathrm{M}}}{\sigma_{\mathrm{c}}}\right)^{m+1}\right] - 1 + \frac{1}{2}P(T_{\mathrm{M}})\right\} - T^{\mathrm{U}}\frac{1-P(T_{\mathrm{M}})}{P(T_{\mathrm{M}})}. \quad (8)$$

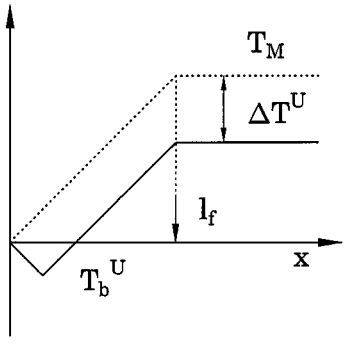

Figure 3 The stress $T_{\mathrm{b}}^{\mathrm{U}}$ along a broken fiber during unloading the specimen (full line). The dotted line indicates the stress distribution before unloading $T_{\mathrm{b}}^{\mathrm{L}}$, and T_{M} denotes the maximal stress reached before the unloading starts. The unloading process is parameterized by ΔT^{U} such that the stress T^{U} in unbroken fibers is $T^{\mathrm{U}} = T_{\mathrm{M}} - \Delta T^{\mathrm{U}}$. In the curve of $T_{\mathrm{b}}^{\mathrm{U}}$ the absolute value of the slope of each straight part is $2\tau/r$.

The constitutive behavior for the unloading case can be obtained substituting Equation 8 into the general form Equation 4 and employing $T^{\mathrm{U}} = E_f \epsilon^{\mathrm{U}}$, where ϵ^{U} denotes the average strain during unloading

$$\frac{\sigma^{\mathrm{U}}}{f} = 2T_{\mathrm{M}}\left(\frac{\sigma_{\mathrm{c}}}{T_{\mathrm{M}}}\right)^{m+1}\left\{ \exp\left[-\left(\frac{\Delta T^{\mathrm{U}}}{2T_{\mathrm{M}}}\right) \times \left(\frac{T_{\mathrm{M}}}{\sigma_{\mathrm{c}}}\right)^{m+1}\right] - 1 + \frac{1}{2}P(T_{\mathrm{M}})\right\}, \quad (9)$$

and in terms of strain

$$\frac{\sigma^{\mathrm{U}}}{f} = 2E_f\epsilon_{\mathrm{M}}\left(\frac{\sigma_{\mathrm{c}}}{E_f\epsilon_{\mathrm{M}}}\right)^{m+1}\left\{ \exp\left[-\left(\frac{\epsilon_{\mathrm{M}} - \epsilon^{\mathrm{U}}}{2\epsilon_{\mathrm{M}}}\right) \times \left(\frac{E_f\epsilon_{\mathrm{M}}}{\sigma_{\mathrm{c}}}\right)^{m+1}\right] - 1 + \frac{1}{2}P(T_{\mathrm{M}})\right\}. \quad (10)$$

Here ϵ_{M} denotes the maximal strain reached before unloading, i.e. $T_{\mathrm{M}} = E_f\epsilon_{\mathrm{M}}$. Note that it is assumed implicitly that during unloading no new fiber breaking can occur. ΔT^{U} takes its largest value T_{m} at complete unloading $\sigma^{\mathrm{U}} = 0$, for which Equation 9 yields

$$T_{\mathrm{m}} = -2T_{\mathrm{M}}\left(\frac{\sigma_{\mathrm{c}}}{T_{\mathrm{M}}}\right)^{m+1}\ln\left[1 - \frac{1}{2}P(T_{\mathrm{M}})\right]. \quad (11)$$

It can be seen from Equation 10 that at complete unoading the specimen $\sigma^{\mathrm{U}} = 0$ remaining anelastic strain ϵ_{an} occurs. From Equations 10 and 11 one obtains

$$\epsilon_{\mathrm{an}} = \epsilon_{\mathrm{M}}\left\{1 + 2\left(\frac{\sigma_{\mathrm{c}}}{E_f\epsilon_{\mathrm{M}}}\right)^{m+1}\ln\left[1 - \frac{1}{2}P(T_{\mathrm{M}})\right]\right\}, \quad (12)$$

which is a function of the maximum strain ϵ_{M} reached before unloading and of the amount of damage $P(T_{\mathrm{M}})$. The non-linear characteristics of ϵ_{an} as a function of ϵ_{M} is illustrated in Fig. 4. It can be seen that ϵ_{an} is roughly one order of magnitude smaller than ϵ_{M}.

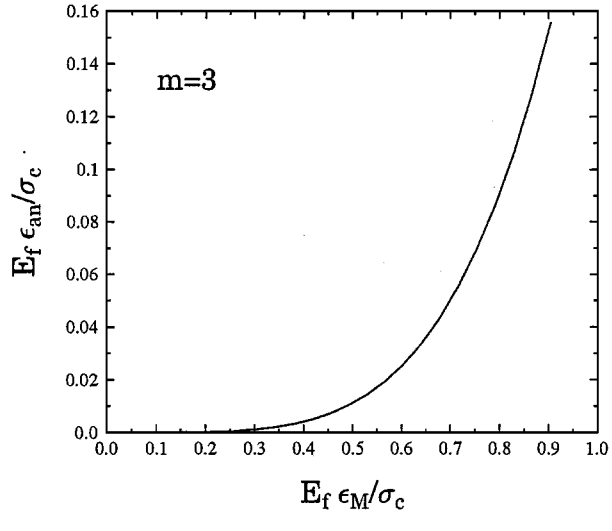

Figure 4 Normalized anelastic strain $E_f\epsilon_{\mathrm{an}}/\sigma_{\mathrm{c}}$ obtained from Equation 12 as a function of the normalized maximal strain $E_f\epsilon_{\mathrm{M}}/\sigma_{\mathrm{c}}$ reached before unloading.

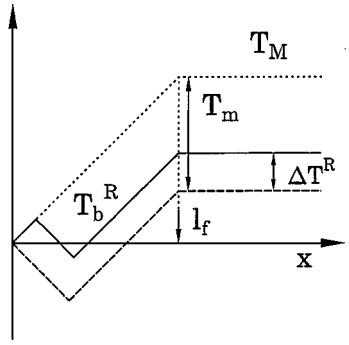

Figure 5 The stress T_b^R along a broken fiber during reloading the specimen (full line). The dotted line indicates the stress before unloading T_b^L, while the dashed line shows the stress distribution T_b^U in the most unloaded situation from which reloading starts. The reloading procedure is parameterized by ΔT^R such that the stress T^R in unbroken fibers is $T^R = T_M - T_m + \Delta T^R$. In the curve of T_b^R the absolute value of the slope of each straight part is $2\tau/r$.

The treatment of reloading is similar. When reloading, the stress T_b^R along broken fibers changes, since the direction of sliding at the broken face switches again to the opposite direction. The reloading process is parameterized by ΔT^R such that the actual stress T^R on intact fibers is $T^R = T_M - T_m + \Delta T^R$, where $\Delta T^R \in [0, T_m]$ [25, 30] (see also Fig. 5). The average value of the stress on broken fibers reads as

$$\langle T_b^R \rangle = \frac{2T_M}{P(T_M)}\left(\frac{\sigma_c}{T_M}\right)^{m+1}\left\{\exp\left[-\left(\frac{T_m}{2T_M}\right)\left(\frac{T_M}{\sigma_c}\right)^{m+1}\right] - \exp\left[-\left(\frac{\Delta T^R}{2T_M}\right)\left(\frac{T_M}{\sigma_c}\right)^{m+1}\right] + \frac{1}{2}P(T_M)\right\} - T^R\frac{1-P(T_M)}{P(T_M)}, \quad (13)$$

and the constitutive behavior can be obtained in the following form

$$\frac{\sigma^R}{f} = 2E_f\epsilon_M\left(\frac{\sigma_c}{E_f\epsilon_M}\right)^{m+1}\left\{1-\left(1-\frac{1}{2}P(T_M)\right)\times\exp\left[-\left(\frac{\epsilon^R-\epsilon_M}{2\epsilon_M}\right)\left(\frac{E_f\epsilon_M}{\sigma_c}\right)^{m+1}\right]\right\}. \quad (14)$$

Loading-unloading-reloading sequences determined by Equations 7, 10 and 14 are presented in Fig. 6. It can be observed that the constitutive behavior is non-linear and for unloading-reloading hysteresis loops occur with decreasing unloading modulus E and increasing opening. In order to characterize the hysteresis loops we calculated the unloading modulus E and the maximum opening $\Delta\epsilon$ of the loops as a function of the maximum strain ϵ_M and the corresponding stress T_M

$$E = fE_f\frac{-P(T_M)}{2\ln\left[1-\frac{1}{2}P(T_M)\right]}, \quad (15)$$

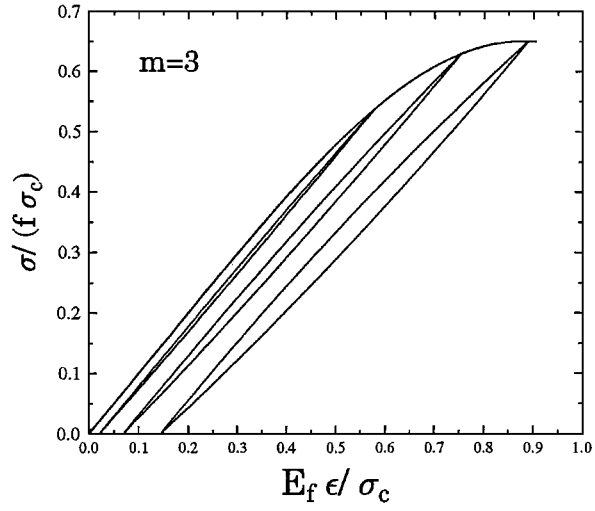

Figure 6 The constitutive behavior determined by Equations 7, 10 and 14. Normalized stress as a function of normalized strain. It can be observed that during unloading-reloading the specimen hysteresis loops occur with decreasing unloading modulus and increasing opening.

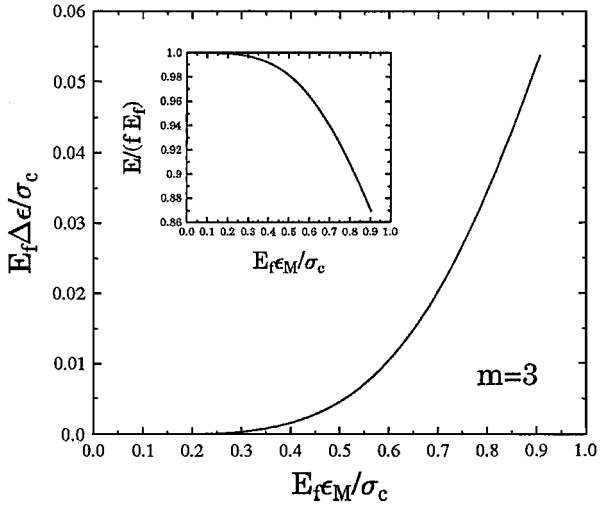

Figure 7 Characterization of the hysteresis loops. Normalized maximum opening $E_f\Delta\epsilon/\sigma_c$ obtained from Equation 15, and the ratio of the unloading modulus E and the initial Young modulus of the specimen fE_f obtained from Equation 16 as a function of the normalized maximal strain $E_f\epsilon_M/\sigma_c$ reached before unloading.

$$\Delta\epsilon = 2\epsilon_M\left(\frac{\sigma_c}{E_f\epsilon_M}\right)^{m+1}\ln\left[\frac{(4-P(T_M))^2}{8(2-P(T_M))}\right]. \quad (16)$$

For illustration see Fig. 7. It has to be emphasized that the non-linear character of the system during unloading and reloading is due to the effect of broken fibers, i.e. due to the second term of Equation 4. In the framework of dry bundle models [1–5, 32–35], where the effect of broken fibers and the materix material is omitted, the behavior of the system under unloading-reloading is completely linear and reversible, anelastic strain or hysteresis cannot appear. An extension of the dry bundle model to account for plastic effects was carried out by Krajcinovic [3].

4. Potential drop

To describe the results of the DC drop measurement it is reasonable to assume that the matrix material does not

contribute to the overall conductivity of the sample, only the fibers are conducting, and hence, the reason for the non-linear increase of the potential drop as a function of the strain is the non-linear reduction of the conducting area due to the gradual breaking of fibers. In order to explain the hysteresis loops of ΔU occurring during the unloading-reloading sequences we suppose that not all the broken fibers are electrically insulating, but it can also happen that fibers which are mechanically disconnected are still conducting due to the closing of cracks. We make the assumption that the number of insulating fibers is proportional to the number of broken fibers and to the average crack opening displacement.

It has been shown in the preceding section that for the constitutive behavior and strength of the composite the relevant length scale is δ_c. However, for the electric resistance, the relevant length scale is the length L_o of the specimen. For the derivation of the electric resistance the specimen can be treated as a series of segments of length δ_c and of number $n = L_o/\delta_c$. Since $P(T)$ provides the probability of fiber breaking in a single segment, the probability $P_{L_o}(T)$ that a fiber of length L_o and of number of segments n breaks at a load less than or equal to T, (i.e. at least one break occurs along the fiber), can be written as

$$P_{L_o}(T) = 1 - (1 - P(T))^n. \tag{17}$$

Using the expression of $P(T)$ Equation 2, P_{L_o} can be cast in the following expression

$$P_{L_o}(T) = 1 - \exp\left[-\frac{L_o}{\delta_c}\left(\frac{T}{\sigma_c}\right)^{m+1}\right], \tag{18}$$

which has the same functional form as $P(T)$.

The electric resistance $R(\epsilon)$ of the specimen can be expressed as

$$R(\epsilon) = \rho\frac{L(\epsilon)}{A(\epsilon)} = \rho\frac{L(\epsilon)}{N_{cond}(\epsilon)A_f(\epsilon)}, \tag{19}$$

where ρ denotes the specific resistance of the fiber material, $L(\epsilon)$ is the actual length of a fiber at a given strain ϵ, and $A(\epsilon)$ denotes the total conducting cross sectional area of the specimen. The second part of Equation 19 demonstrates that the reduction of the conducting area A with increasing load is due to two reasons. On the one hand, the elongation of the specimen gives rise to decrease of the cross section of the individual fibers A_f due to their non-zero Poisson ratio. On the other hand, the subsequent breaking of fibers under gradual loading results in further reduction of the conducting area. $N_{cond}(\epsilon)$ designates the number of conducting fibers, for which we introduce the following form

$$N_{cond}(\epsilon) = N - \frac{\Delta l(\epsilon)}{\Delta l_c} N P_{L_o}(T_M), \tag{20}$$

where $\Delta l(\epsilon)$ denotes the crack opening displacement, and Δl_c is the critical value of Δl reached at ultimate failure. In Equation 20 the term $NP_{L_o}(T_M)$ yields the average number of broken fibers, i.e. the average number of fibers with at least one broken segment. The prefactor $\Delta l(\epsilon)/\Delta l_c \leq 1$ implies that a certain fraction of broken fibers still remains conducting.

The prefactor $\Delta l(\epsilon)/\Delta l_c$ plays a crucial role during unloading and reloading. It has been assumed that no damage occurs during the unloading-reloading sequences, i.e. in this regime the value of $P_{L_o}(T_M)$ is constant, and consequently, the electric resistance varies due to the deformation of fibers and due to the closing and opening of cracks captured by the change of $\Delta l(\epsilon)/\Delta l_c$. For simplicity, in the derivation of $R(\epsilon)$ we neglect that the electric resistance due to the closing of cracks can depend on the actual stress, and generally it is higher than the resistance of intact fibers.

Assuming linear elastic behavior for fibers their length $L(\epsilon)$ and cross section $A_f(\epsilon)$ can be obtained as

$$L(\epsilon) = L_o(1 + \epsilon), \tag{21}$$

$$A_f(\epsilon) = A_{fo}(1 - 2\nu\epsilon), \tag{22}$$

and the potential drop reads as

$$U(\epsilon) = I_o\rho\frac{L(\epsilon)}{N_{cond}(\epsilon)A_f(\epsilon)}. \tag{23}$$

where ν designates the Poisson ratio of fibers, and I_o is the fixed electric current maintained on the sample. Finally, ΔU can be expressed as

$$\Delta U = U(\epsilon) - U_o = U_o\left[\frac{(1+\epsilon)(1+2\nu\epsilon)}{1 - \frac{\Delta l(\epsilon)}{\Delta l_c}P_{L_o}(T_M)} - 1\right], \tag{24}$$

where $U_o = I_o\rho L_o/NA_{fo}$ is the potential drop in the initial state.

When the damage is sufficiently small, Equation 24 can be cast into the approximate form, which is easier to analyze

$$\Delta U \approx U_o\left[\epsilon(1+2\nu) + \frac{\Delta l(\epsilon)}{\Delta l_c}P_{L_o}(T_M)\right]. \tag{25}$$

It can be observed that the first term of Equation 25 describes the dependence of ΔU due to stretching of fibers, while the second term is the irreversible contribution of fiber failure. In the absence of fiber breaking, ΔU would be a linear function of ϵ and it would behave reversible during the unloading-reloading sequences. Non-linearity arises due to fiber breaking and the sliding fiber-matrix interface. The relative importance of the two mechanisms, i.e. deformation and damage, changes at a crossover strain ϵ_{cr} where $\epsilon_{cr}(1+2\nu) = (\Delta l(\epsilon_{cr})/\Delta l_c)P_{L_o}(E_f\epsilon_{cr})$. For deformations $\epsilon \ll \epsilon_{cr}$ the linear term is relevant, while for $\epsilon > \epsilon_{cr}$ the second term dominates the sum giving rise to a non-linear increase and hysteresis during unloading-reloading. In the completely unloaded case the electric resistance is determined by the damage $P_{L_o}(T_M)$, by the remaining anelastic deformation ϵ_{an}, and by the closing of cracks desribed by $\Delta l/\Delta l_c$.

Following Ref. [25] the crack opening displacement Δl can be defined as the displacement difference between a broken face and an adjacent unbroken fiber, i.e.

$$\Delta l = l_f \frac{T - \langle T_b \rangle}{E_f} = \frac{r T (T - \langle T_b \rangle)}{2\tau E_f}. \quad (26)$$

The specific forms of Δl for the case of loading, unloading and reloading can be obtained by substituting Equations 6, 8 and 13 into the general form Equation 26.

$$\Delta l^{\mathrm{L}} = B(\epsilon^{\mathrm{L}})^2 \left[1 - P(T_{\mathrm{M}}) \left(\frac{\sigma_{\mathrm{c}}}{T_{\mathrm{M}}} \right)^{m+1} \right], \quad (27)$$

$$\Delta l^{\mathrm{U}} = B\epsilon_{\mathrm{M}} \left\{ \epsilon^{\mathrm{U}} - 2\epsilon_{\mathrm{M}} \left(\frac{\sigma_{\mathrm{c}}}{T_{\mathrm{M}}} \right)^{m+1} \times \left[\exp\left[-\left(\frac{\epsilon_{\mathrm{M}} - \epsilon^{\mathrm{U}}}{2\epsilon_{\mathrm{M}}} \right) \left(\frac{T_{\mathrm{M}}}{\sigma_{\mathrm{c}}} \right)^{m+1} \right] - 1 + \frac{1}{2} P(T_{\mathrm{M}}) \right] \right\}, \quad (28)$$

$$\Delta l^{\mathrm{R}} = B\epsilon_{\mathrm{M}} \left\{ \epsilon^{\mathrm{R}} - 2\epsilon_{\mathrm{M}} \left(\frac{\sigma_{\mathrm{c}}}{T_{\mathrm{M}}} \right)^{m+1} \times \left[1 - \left(1 - \frac{1}{2} P(T_{\mathrm{M}}) \right) \times \exp\left[-\left(\frac{\epsilon^{\mathrm{R}} - \epsilon_{\mathrm{M}}}{2\epsilon_{\mathrm{M}}} \right) \left(\frac{T_{\mathrm{M}}}{\sigma_{\mathrm{c}}} \right)^{m+1} \right] \right] \right\}, \quad (29)$$

where the common multiplication factor is $B = r E_f / (2\tau P(T_{\mathrm{M}}))$. Finally, the potential drop ΔU is characterized by Equations 24, 25 and 27–29. It has to be emphasized that the form of Δl^{U} and Δl^{R} results in hysteresis loops of ΔU during unloading-reloading.

5. Comparison to experiments

In the present chapter the constitutive behavior determined by Equations 7, 10 and 14 and the potential drop described by Equations 24, 25 and 27–29 of the model will be compared to the experimental results. The measured values of the most important characteristic quantities of the constituent fibers and that of the C/C-SiC composite are summarized in Table I.

TABLE I The parameter values

Parameter	Symbol	Unit	Value
Young modulus of C fibers	E_f	GPa	230
Characteristic strength of C fibers	σ_{o}	MPa	3530
Weibull modulus of C fibers	m	1	3.3 ± 0.6
Young modulus of composite	E	GPa	70–80
Ultimate tensile strength of composite	σ_{UTS}	MPa	90–170
Volume fraction of fibers	f	1	0.32
Initial potential drop	U_{o}	mV	185

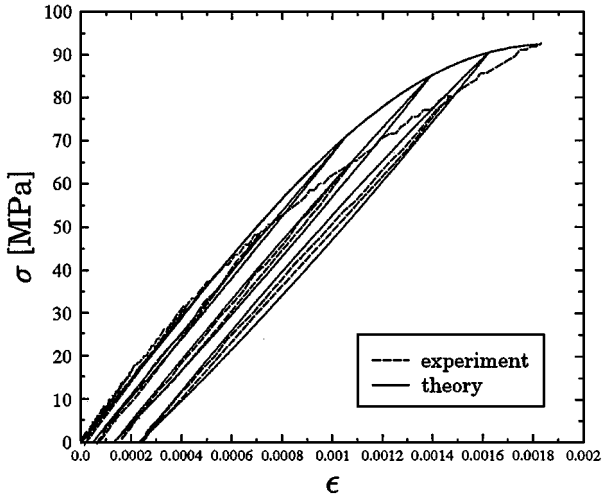

Figure 8 Comparison of the constitutive behavior determined by Equations 7, 10 and 14 to the experimental results. The values of the fitting parameters are $\sigma_{\mathrm{c}} = 460$ MPa and $m = 1.85$. For the other parameters see Table I.

According to the experiments, during the manufacturing process of the composite not only the matrix material gets multiply cracked but a certain fraction of fibers also breaks [19–24]. This initial damage of fibers and its effect on the development of damage under loading is very hard to quantify. Furthermore, our model calculation is based on the assumption of global load sharing. It is well known about GLS that it over estimates the ultimate tensile strength σ_{UTS} of composites, since it neglects stress concentration around failed fibers. Due to these reasons the constitutive behavior was fitted such that the volume fraction f and the Young modulus E_f of fibers were considered as input parameters from Table I, and the value of the characteristic strength σ_{c}, and the Weibull modulus m of fibers were varied until best fit was achieved. The product fE_f gives the Young modulus of the composite in the initial state, i.e. the initial slope of the loading curve. Hence, in the fitting this has to be fixed and the shape of the theoretical curve Equations 7, 10 and 14 is controlled only by σ_{c} and m. The result of the fitting procedure is presented in Fig. 8. The values of the fitting parameters are $\sigma_{\mathrm{c}} = 460$ MPa and $m = 1.85$. It can be observed in Fig. 8 that the quality of the fit is satisfactory, there is larger deviation only in the vicinity of global failure. In this region the experimental curve is more brittle in the sense that it is practically straight, while the fitted curve has a certain curvature. Using a sophisticated simulation technique, it was shown in Ref. [14] that decreasing the range of stress redistribution, i.e. making load sharing more and more localized, the ultimate tensile strength σ_{UTS} decreases and the overall constitutive behavior of the composite becomes more brittle. Hence, it is reasonable to assume that the discrepancy between the fitted and the experimental curve is due to the neglect of possible stress localization. The value of σ_{c} obtained from the fitting procedure cannot be compared to σ_{o} in Table I, because in the experiments the sliding resistance τ was not measured.

Since the value of δ_{c} cannot be determined in the absence of τ, for the fitting of the potential drop we set the

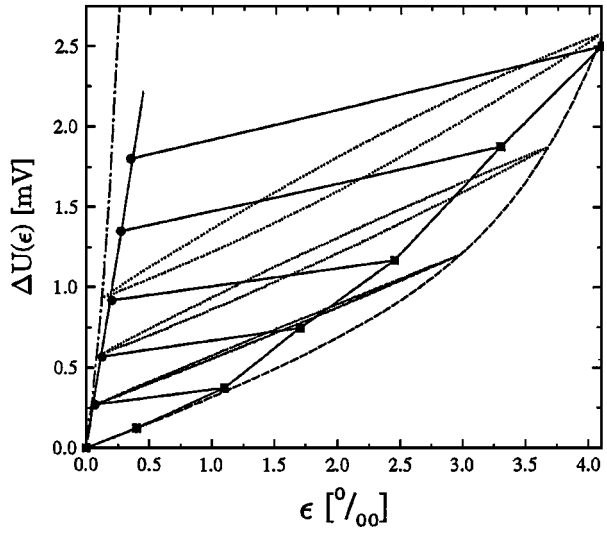

Figure 9 Comparison of the potential drop determined by Equations 24, 25 and 27–29 to the experimental results. Experimental results: full square: loading, full circle: complete unloading. Theoretical results: dashed line: loading, dotted-line: unloading-reloading sequences, dashed-dotted line: complete unloading. The value of the fitting parameters are $\sigma_c = 1900$ MPa and $m = 1.8$. For the other parameters see Table I.

value of $n = L_o/\delta_c$ to 1 in Equations 24 and 25. Then, the potential drop Equations 24, 25 and 27–29 can be fitted to the experimental results in such a way that the value of the potential drop U_o measured in the initial state, the Young modulus E_f and Poisson ratio ν of fibers are considered as input parameters and again σ_c and m control the overall shape of the theoretical curve. Note that U_o determines the slope of ΔU in the vicinity of $\epsilon \sim 0$. The best fit obtained is presented in Fig. 9. It can be observed that the model calculations are in reasonable agreement with the experimental results. The value of the fitting parameters are $\sigma_c = 1900$ MPa and $m = 1.8$. This value of σ_c is different from the value obtained by fitting the constitutive behavior, since the two experiments were carried out on different specimens having different values of failure strength. The values of m obtained from the two fittings agree fairly well.

It was found in the experiments that the potential drop measured during loading (full squares in Fig. 9) can be well fitted with a power law, i.e. $\Delta U \approx \epsilon^a$. The value of the exponent a scatters between 1 and 2 depending on the sample, and it is $a = 1.42$ for the specific case presented in Fig. 9. The theoretical curve can also be approximated with a power law with an exponent 1.54, which is consistent with the experimental result. In the case of complete unloading the experimental data (full circles) were fitted with a straight line. The theoretical curve (dashed-dotted line) seems to agree with this functional behavior. The unloading-reloading curves in Fig. 9 are somewhat steeper than the experimentally observed ones. In our calculations those fibers in the woven structure, which are perpendicular to the load direction were completely omitted. However, it can also happen that there are conducting contacts between fibers perpendicular to each other. This effect is difficult to quantify, but it can be partly responsible for slight discrepancies of the theory and the experiments. Furthermore, we neglected that the electric resistance due to the closing of cracks can depend on the actual stress level, and in general, it is higher than the resistance of intact fibers. The value of $n = L_o/\delta_c$, which was set to 1 for the fitting, can also slightly affect the shape of the theoretical curves but not the overall functional behavior.

The experimental results obtained with different specimens show a statistical variation, since the behavior of the material strongly depends on the microstructure controlled by the manufacturing process. Since our model is based on average quantities, the fitting of different experiments result in a certain variation of the fitting parameters.

6. Discussion

In the present paper we made an attempt to give a theoretical interpretation of the experimental results concerning the damage development in the C/C-SiC composite under uniaxial cyclic loading-unloading-reloading. Our approach is based on statistical micromechanical models of the failure of composites, and captures quasi-periodic matrix cracking, gradual breaking of fibers and sliding of fibers relative to the matrix as failure mechanism within a global load sharing framework. The constitutive behavior of the material and the potential drop was reproduced by the model calculations with a reasonable accuracy. The theoretical results are general, they can be applied to study the behavior of other composites as well.

The question naturally arises whether it is possible to introduce a damage variable in terms of the potential drop ΔU. It follows from our treatment that in simple cases the damage occurring in fiber bundles can be fully characterized by ΔU measured during the loading process, however, in more realistic situations it can happen that the electric resistance of the specimen is also strongly affected by matrix cracking occurring in both the transversal and longitudinal plys, and by the complicated conducting contacts between the fibers of the woven plys. In these cases the measurement of the potential drop does not provide sufficient information for the characterization of damage.

The main limitation of the present approach is the assumption of global load sharing. Besides the possible effects of localized load sharing mentioned in the paper, microstructural analysis of damaged specimens showed that the microcracks occurring in fiber bundles have an interesting spatial distribution [23], which cannot be understood in a global load sharing framework due to the neglect of any spatial correlations. Furthermore, the internal geometry of the composite has a hierarchical structure, i.e. the fibers are organized into subbundels, the subbundles form bundles, then plies, and finally the specimen is built up from plies. This hierarchical organization shows up also in the damage development in the composite. That is why, for a quantitative grasp of these phenomena, it is necessary to work out a scale dependent description, based on real space renormalization, in the framework of local load sharing.

To describe more complicated loading situations occurring in practical applications (e.g. multiaxial load) our method has to be improved by taking into account

both plys (the transversal and the longitudinal one) with a proper coupling in between. In these loading cases additional damage mechanisms are activated (matrix cracking, delamination, debonding) interacting with each other, the treatment of which is rather complicated. Further experimental and theoretical investigations in this direction are in progress.

Recently, it has been shown that the size distribution of avalanches of fiber breaks in dry fiber bundle models shows universal power law behavior [32–35]. From the view point of statistical physics, it would be very interesting to see how robust the universality is with respect to the effect of matrix material, which can be studied in the model presented here.

Acknowledgement

We are very grateful to A. Udoh, D. Walz, K. Maile, and R. Aoki for sending us preprints of their works and for the valuable discussions. This work was supported by the project SFB381. F. Kun acknowledges financial support of the Alexander von Humboldt Foundation (Roman Herzog Fellowship) and OTKA T-023844.

References

1. H. E. DANIELS, *Proc. R. Soc. London A* **183** (1945) 405.
2. B. D. COLEMAN, *J. Appl. Phys.* **29** (1958) 968.
3. D. KRAJCINOVIC and M. A. G. SILVA, *Int. J. Solids Struct.* **18** (1982) 551.
4. D. SORNETTE, *J. Phys. A* **22** (1989) L243.
5. *Idem., J. Phys. France* **50** (1989) 745.
6. C. MOUKARZEL and P. M. DUXBURY, *J. Appl. Phys.* **76** (1994) 1.
7. D. G. HARLOW and S. L. PHOENIX, *J. Composite Mater.* **12** (1978) 195.
8. R. L. SMITH and S. L. PHOENIX, *J. Appl. Mech.* **48** (1981) 75; D. G. HARLOW and S. L. PHOENIX, *J. Mech. Phys. Solids* **39** (1991) 173.
9. S. L. PHOENIX, M. IBNABDELJALIL and C.-Y. HUI, *Int. J. Solids Struct.* **34** (1997) 545.
10. S. L. PHOENIX and RAJ, *Acta Metall. Mater.* **40** (1992) 2813.
11. I. J. BEYERLEIN and S. L. PHOENIX, *J. Mech. Phys. Solids* **44** (1996) 1997.
12. M. IBNABDELJALIL and W. A. CURTIN, *Int. J. Solids Struct.* **34** (1997) 2649.
13. W. A. CURTIN, *J. Mech. Phys. Solids* **41** (1993) 217.
14. S. J. ZHOU and W. A. CURTIN, *Acta. Metal. Mater.* **43** (1995) 3093.
15. W. A. CURTIN and N. TAKEDA, *J. Comp. Matls.* **32** (1998) 2042.
16. W. A. CURTIN, *J. Am. Ceram. Soc.* **74** (1991) 2837.
17. *Idem., Phys. Rev. Lett.* **80** (1998) 1445.
18. A. G. EVANS and F. W. ZOK, *J. Mater. Sci.* **29** (1994) 3857.
19. D. WALZ, Arbeits- und Ergebnisbericht 1996 des SFB 381-Teilprojektes A4 (Stuttgart, Germany, 1996).
20. K. MAILE, K. KUSSMAUL and D. S. WALZ, in Proceedings of 5th International Conference on Composites Engineering, Las Vegas, July 1997.
21. K. MAILE and D. WALZ, in Proceedings of 4th International Conference on Ceramic Composites, Belgium, November 1997.
22. A. UDOH and K. MAILE, Preprint, unpublished.
23. *Idem.*, Preprint, unpublished.
24. R. AOKI, Preprint, unpublished.
25. F. HILD, A. BURR and F. A. LECKIE, *Eur. J. Mech. A* **13** (1994) 731.
26. N. WEIGEL, B. KRÖPLIN and D. DINKLER, unpublished.
27. P. LADEVÈZE, A. GASSER and O. ALLIX, *J. Engineering Materials and Technology* **116** (1994) 331.
28. H. CAO and M. D. THOULESS, *J. Am. Ceram. Soc.* **73** (1990) 2091.
29. K. R. TURNER, J. S. SPECK and A. G. EVANS, *ibid.* **78** (1995) 1841.
30. D. B. MARSHALL and W. C. OLIVER, *ibid.* **70** (1987) 542.
31. H. L. COX, *Br. J. Appl. Phys.* **3** (1952) 72.
32. A. HANSEN and P. C. HEMMER, *Phys. Lett. A* **184** (1994) 394.
33. M. KLOSTER, A. HANSEN and P. C. HEMMER, *Phys. Rev. E* **56** (1997) 2615.
34. W. I. NEWMAN, A. M. GABRIELOV, T. A. DURAND, S. L. PHOENIX and D. L. TURCOTTE, *Physica D* **77** (1994) 200.
35. W. I. NEWMAN, D. L. TURCOTTE and A. M. GABRIELOV, *Phys. Rev. E* **52** (1995) 4827.

Received 12 May 1999
and accepted 3 March 2000